PHYSICAL REVIEW A **80**, 031804(R) (2009)

Optical turbulence and spectral condensate in long-fiber lasers

Elena G. Turitsyna,[1] Gregory Falkovich,[2] Vladimir K. Mezentsev,[1] and Sergei K. Turitsyn[1]
[1]*Photonics Research Group, Aston University, Birmingham B4 7ET, United Kingdom*
[2]*Physics of Complex Systems, Weizmann Institute of Science, Rehovot 76100, Israel*
(Received 16 February 2009; published 22 September 2009)

We study optical wave turbulence using as a particular example recently created ultralong-fiber laser. We show that the sign of the cavity dispersion has a critical impact on the spectral and temporal properties of generated radiation that are directly relevant to the fiber laser performance. For a normal dispersion, we observe an intermediate state with an extremely narrow spectrum (condensate), which experiences an instability and a sharp transition to a strongly fluctuating regime with a wide spectrum and increased probability of spontaneous generation of large-amplitude pulses.

DOI: 10.1103/PhysRevA.80.031804 PACS number(s): 42.65.Sf, 42.55.Ah, 42.55.Wd, 47.27.Gs

Powerful fiber laser presents both an interesting nonlinear physical system and a photonic device with an incredible range of practical applications (in telecommunications, medicine, metrology, spectroscopy, sensing, industrial cutting, welding, and others). The Raman fiber laser exploits the effect of simulated Raman scattering to shift the generated spectrum from pumping toward longer wavelengths. Using several frequency conversion cascades based on Stokes lines resonating in nested cavities, the pump power (e.g., easily available around 1 μm) can be shifted deep into the longer wavelength region. Of a particular interest is an ability to fully cover the spectral region near telecommunication windows of transparency, making Raman fiber lasers very attractive pump sources for a distributed Raman amplification that is one of important enabling technologies in high-speed optical communication [1–5]. Using fiber Bragg gratings (FBGs) as cavity reflectors at the Stokes wavelength, it is possible to achieve lasing in a fiber waveguide with the length L of the order of several kilometers [6]. The quasilossless fiber span with highly reduced power variations during transmission can be implemented using symmetric second-order pumping schemes leading to the concept of ultralong fiber lasers [7–10], which promises new applications in transmission and secure communication [11]. Raman fiber lasers are also attractive continuous light sources for optical coherence tomography [12], long-distance remote sensing [13], as a source for the laser guide star for the mesospheric sodium layer [14], and other applications (see, e.g., [15]). Despite existing and emerging practical applications of such lasers, some fundamental physical phenomena underlying their operation and nonlinear mechanisms determining properties of generated radiation are not yet fully understood.

In this paper, we demonstrate the impact of optical wave turbulence on spectra and coherence of radiation generated in fiber lasers. Understanding these key properties is very important for practice and at the same time presents a fundamental physical problem. A long cavity of a fiber laser provides for a very large number (up to 10^8) of interacting modes even for a relatively narrow excitation spectrum. That makes such lasers convenient for studying fundamental problems of nonlinear and nonequilibrium physics: modulational instability, optical turbulence, and interaction of spectral condensate with turbulence. The precision of measurements available in optical experiments makes a fiber laser an excellent tool for quantitative analysis of dynamical and statistical problems of nonlinear physics.

The standard evolution equation for the longitudinal modes (indexed by m) of the envelope can be derived from the generalized Schrödinger equations for backward and forward Stokes waves [16–18]

$$\frac{\tau_{rt}}{L}\frac{dE_m}{dt} = (G_m + i\beta_2\Omega_m^2)E_m - i\gamma\sum E_i E_k E^*_{i+k-m}. \qquad (1)$$

Here, the round-trip time is $\tau_{rt}=2Ln/c$, L is the cavity length, c/n is the speed of light (we use $n=1.45$), and $G_m=g-\delta_m/L$ describes the effective pumping $g(P)$ which is a decreasing function of the total generated power $P\equiv\Sigma|E_m|^2$ and the damping δ_m which is a growing function of m [see definitions around Eq. (2) below]. The group-velocity dispersion coefficient is $\beta_2[\mathrm{ps}^2/\mathrm{km}]$ and $\Omega_m \propto m$.

In treating a very large number of interacting modes sharing between them a finite generated power, it seemed a natural first step to assume the interaction weak, the spectrum wide, and the phases of different modes random. This is a weak-turbulence approach described in [19] and applied to fiber lasers in [17,18,20]. Its predictions are insensitive to the sign of wave dispersion β_2. In the present work, however, we find that changing the dispersion sign dramatically changes the spectral shape and the statistics of the laser radiation.

When the effective pumping or dissipation G_m is a decreasing function of both m and P, Eq. (1) has an exact solution: one-mode condensate, $E_m(t)=\sqrt{P}\delta_{m0}\exp(-i\gamma Pt)$, which corresponds (for a given pump) to the maximal P determined by $G_0=0$. Side modes m and $-m$ interact resonantly with the zero mode

$$dE_m/dt = (G_m + i\beta_2\Omega_m^2)E_m - i\gamma P E^*_{-m},$$

$$dE^*_{-m}/dt = (G_m + i\beta_2\Omega_m^2)E^*_{-m} - i\gamma P E_m.$$

That system has an exponential solution E_m, $E^*_{-m}\propto\exp(\nu t)$, with $\nu=G_m-\beta_2\Omega_m^2(\beta_2\Omega_m^2+\gamma P)$. Since $G_m\leq 0$ in a steady state, then only for an anomalous dispersion ($\beta_2<0$), one can have $\nu>0$ which corresponds to a so-called modulational instability (MI). MI broadens the distribution up to the root-mean-square width $\Omega^2_{\mathrm{rms}}\simeq\gamma P/\beta_2$. Indeed, solving Eq. (1) numerically, we observe for $\beta_2<0$ the spectra of such

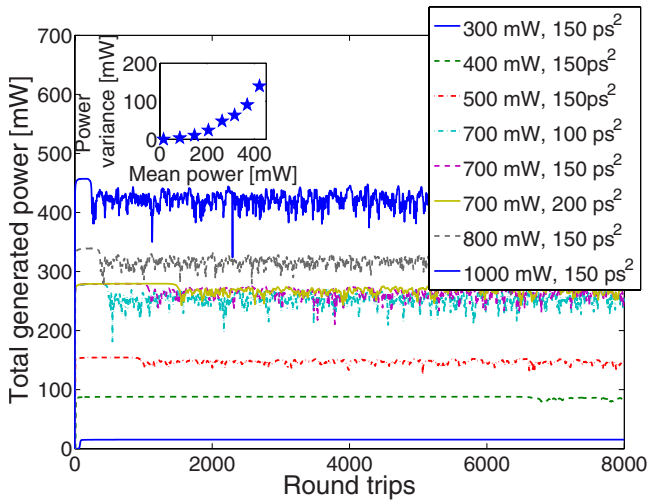

FIG. 1. (Color online) Generated power vs time for different values of dispersion and pump powers. Inset: power variance vs the mean for $\beta_2 L = 150$ ps^2.

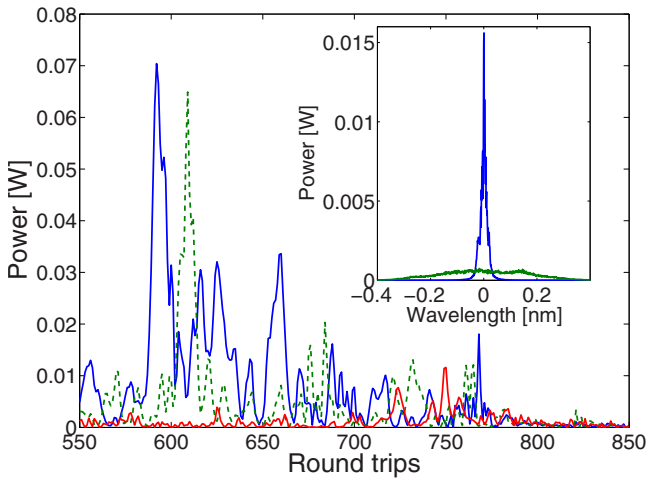

FIG. 2. (Color online) Time dependence of the modes with $n=0$ (blue), $n=5$ (green), and $n=10$ (red). Inset: spectra before and after condensate destruction, averaged between 550 and 650 round trips (blue) and between 850 and 950 round trips (green).

width, which are formed and became steady after few round-trip times.

For a normal dispersion, the one-mode condensate is stable with respect to infinitesimal perturbations. In reality, however, the modes of a long cavity are so spectrally dense that one cannot avoid exciting few side modes too. Nonlinear interaction between these few modes can lead to a complicated evolution including dynamical chaos which may result in side modes amplitudes exceeding that of the zero mode at some instant. That may lead to a further spectrum broadening due to so-called four-wave mixing (FWM) described by nonresonant terms in the sum in Eq. (1). Indeed, for a range of parameters, we observe that the condensate appears, persists for many round trips, and then dissolves into a wider spectrum. That is seen from Fig. 1 that shows the evolution of the generated power for $\beta_2 > 0$. A very narrow condensate of few modes is formed initially. It persists for a time depending on the number of modes and the absolute value of dispersion. While during the condensate lifetime, the total intensity is constant with high accuracy (as seen in Fig. 1), it conceals a rich internal dynamics shown in Fig. 2 (which corresponds to 700 mW and 150 ps^2): the interaction between the few modes of the condensate leads to an irregular evolution of their amplitudes which suggest dynamical chaos. This phenomenon and its relation to the condensate destruction will be addressed elsewhere. The condensate destruction is manifested by a sharp transition to a wider spectrum and a lower mean power. That new (statistically steady) state is accompanied by strong fluctuations which seem to be a sign of bistability. Inset shows how the fluctuation level depends on the power. It is clear that there is no threshold so that the condensate is likely to be metastable at all power levels in that case ($\beta_2 L = 150$ ps^2). The condensate lifetime dramatically increases when the number of modes is small and the dispersion is large; in this case, the dispersion between the frequencies of the adjacent modes is large enough to suppress a nonresonant FWM. For sufficiently small number of modes and high β_2, the condensate persisted for as long as we managed to run the simulations. It is unclear whether it is an asymptotic steady state or just a very long-living metastable state in such cases.

Spectrum broadening at $\beta_2 > 0$ is due to the competition between FWM and dispersion, so that one can expect that the width is determined by the balance of dispersion and nonlinearity, $\beta_2 \Omega_{\mathrm{rms}}^2 \simeq \gamma P$, i.e., comparable to that determined by MI. That would mean that the effective nonlinearity/dispersion ratio $\xi = \gamma P / |\beta_2| \Omega_{\mathrm{rms}}^2$ must stay approximately constant and of order unity. We found that indeed ξ practically does not depend on $|\beta_2| L$ (in the interval 50,300 ps^2) and the pump power (in the interval $2P_0 = 400$, 1000 mW): $\xi \simeq 1.7$ for $\beta_2 < 0$ and $\xi \simeq 3.3$ for $\beta_2 > 0$. It is seen that the spectral width is such that the effective dispersion is almost twice larger for $\beta_2 < 0$ when it must balance both nonlinearities, MI and FWM, acting together to widen the spectrum. Since $\xi > 1$, then in all these cases most of the modes cannot be treated by the weak-turbulence approximation (which is expected to work when $\xi_m = \gamma P / |\beta_2| \Omega_m^2 \ll 1$). That conclusion is further supported by the dramatic differences between the cases of normal and anomalous dispersions as discussed above. Figure 3 shows the average spectra of generated radiation after many round trips. While the integral characteristics such as the root-mean-square spectral width are comparable, the spectra for $\beta_2 < 0$ are smoother and have a characteristic triangular shape with more narrow peaks compared to more concave and irregular spectra for normal dispersion. How an interplay between resonant and nonresonant interactions (MI and FWM) determines so different spectra shapes will be a subject of a future work. The interaction conserves energy so that $\Sigma G_m |E_m|^2 = 0$ in a steady state. Since the effective pumping is a decreasing function of P and m, then the broader the steady-state spectrum, the larger must be an effective pumping and the smaller is P, as indeed seen in Fig. 4.

Temporal coherence of radiation is characterized by the autocorrelation function $K_n(t) = \Sigma_\tau \langle E_n(\tau - t/2) E_n^*(\tau + t/2) \rangle$. Figure 5 shows $K_n(t)$ for negative and positive β_2. The condensate is indeed coherent over many periods while for

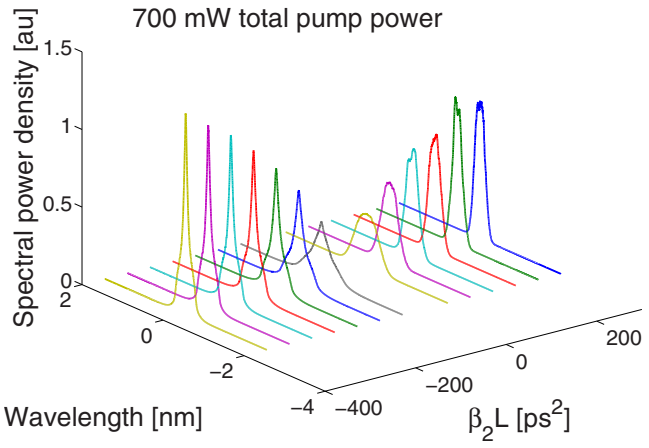

FIG. 3. (Color online) Spectra of generated radiation for different $\beta_2 L$.

broad spectra at both signs of β_2, decorrelation happens at the time scale which is below one round trip.

Fluctuations of the generated power are characterized by histograms in Fig. 6 with the condensate distribution being much narrower than both other histograms. Not surprisingly, the condensate is the state with less fluctuations. Note also that its histogram is very asymmetric with the highest value being most probable which can be naturally interpreted as fluctuations being only "holes" in the condensate (such as gray and dark solitons, see, e.g., [21]). An abrupt decay of the probability of intensities exceeding certain value can be thought of as an interesting effect of nonlinear self-induced optical limiting, which prevents the laser power from random overshoot and might be of a practical importance in power-sensitive applications in laser systems providing for a stable mode condensate. On the contrary, when the condensate is destroyed, the histograms are much wider and more symmetric with substantial probability of fluctuations exceeding mean value. Somewhat unexpectedly, we see that the modulational instability at $\beta_2<0$ broadens the histogram much less than the FWM mixing at $\beta_2>0$ (note that while it is reasonable to assume that MI plays a role in creating so-called rogue waves [22–25], we see here that the destruction

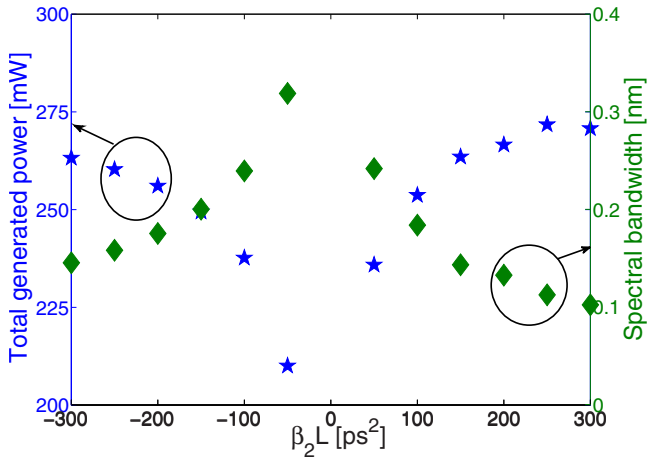

FIG. 4. (Color online) Spectral bandwidth (diamonds) and generated power (stars) vs $\beta_2 L$.

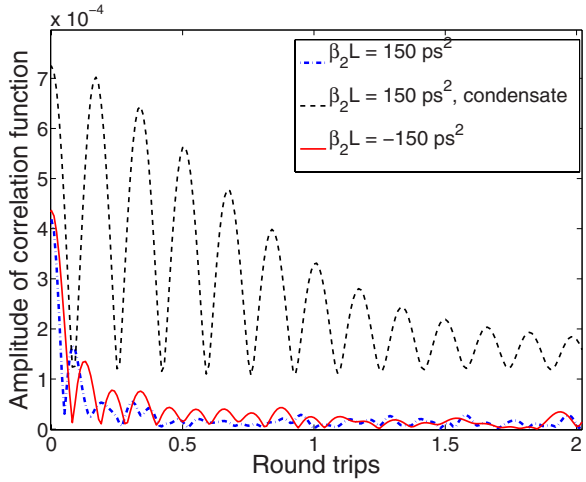

FIG. 5. (Color online) Amplitude correlation functions for the central mode.

of the condensate produces much higher probabilities of large amplitudes when MI is absent). The important practical observation in Fig. 6 is that positive (normal) cavity dispersion provides for much larger amplitude jitters in the generated continuous wave compared to the case of negative (anomalous) dispersion.

Here we list the parameters of the numerics. We used the nonlinearity parameter $\gamma=1.45$ (W km)$^{-1}$ and the effective pumping $g=g_R\bar{P}-\alpha$. Here, $\alpha=0.25/8.66$ km^{-1} is the distributed fiber loss at $\lambda=1455$ nm (Stokes) and $g_R\bar{P}$ is the effective distributed round-trip amplification, which depends on the Raman coefficient $g_R g_R=0.51$ (W km)$^{-1}$ and the pump power $\bar{P}$ averaged over the resonator length (see, e.g., [18])

$$\bar{P} = 2P_0 \frac{1-\exp\{-L[\alpha_P + (\lambda/\lambda_P)g_R P]\}}{L[\alpha_P + (\lambda/\lambda_P)g_R P]}. \tag{2}$$

We considered a symmetric pumping scheme described in [8,10,20], where $2P_0$ being the input pump power and $\alpha_P=0.31/8.66$ km^{-1} is the distributed loss at the pump wave-

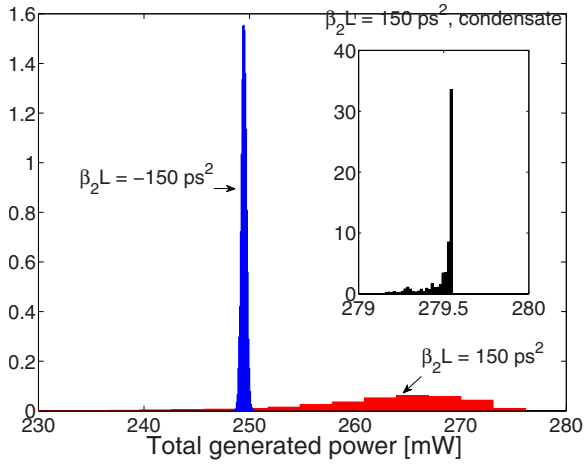

FIG. 6. (Color online) Histograms of total generated power for normal and anomalous dispersions.

length $\lambda_P=1365$ nm. We put $\Omega_m=m\Delta$, where $\Delta=\Omega/M$ is a spectral separation between modes, Ω is the total spectral interval, and M is the total number of modes used in numerical modeling. The window of $\Lambda=\lambda^2\Omega/(2\pi c)=8$ nm significantly exceeded the spectral width in all cases. We used $M=2^{13}$ modes and have verified that changing it up to 2^{16}, decreasing time steps or increasing the window do not affect the results. δ_m describes the combined effect of all lumped losses and the frequency-dependent FBG losses. We use $\delta_m=0.3+\delta_2(m\Delta)^2=0.3+\delta_2[\mathrm{nm}^{-2}](m\Lambda/M)^2$ (corresponding to a Gaussian spectral response of the FBGs) with $\delta_2[\mathrm{nm}^{-2}]=3$ nm^{-2}. We used $L=22$ km and the variety of $\beta_2 L$ values from -300 to 300 ps^2 (for a single mode fiber with $L=22$ km $\beta_2 L=-250$ ps^2). Input pump power for Figs. 3–6 is 700 mW for all values of $\beta_2 L$.

We have here a true multimode turbulence with a wide transparency window since for most m within the spectrum δ_m is much less than the effective nonlinearity γP, which is comparable to the effective pumping g and dispersion $\beta_2\Omega_{\mathrm{rms}}^2$ for all values of parameters. We do not expect, however, any turbulence cascades since the interaction is nonlocal in m.

To conclude, we have demonstrated that the sign of cavity dispersion has dramatic impact on optical turbulence that determines the spectral and temporal properties of generated radiation, directly related to the performance of an ultralong fiber laser. For a normal dispersion, we observe an intermediate state with an extremely narrow spectrum (condensate) that experiences an instability and a sharp transition to a strongly fluctuating regime. Power histograms show that normal dispersion increases the probability of spontaneous generation of large-amplitude pulses—optical rogue waves. For an anomalous dispersion, we have observed triangular spectra and more coherent temporal behavior of generated radiation.

We acknowledge the support of the Royal Society, EPSRC-GB, the Israel Science Foundation, and the Minerva Einstein Center at WIS.

[1] R. Stolen and E. Ippen, Appl. Phys. Lett. **22**, 276 (1973).
[2] L. F. Mollenauer, J. P. Gordon, and M. N. Islam, IEEE J. Quantum Electron **22**, 157 (1986).
[3] S. V. Chernikov, A. E. Lewis, and J. R. Taylor, OFC'1999, 1999 (unpublished).
[4] C. Headley and G. Agrawal, *Raman Amplification in Fibre Optical Communication Systems* (Academic Press, New York, 2004).
[5] M. Vasilyev, Proceedings of the Optical Fibre Conference 2003, OSA Anaheim, USA, 2003, p. 303; S. B. Papernyi, V. J. Karpov, and W. R. L. Clements, Proceedings of the Optical Fibre Conference 2002, OSA, Anaheim, USA, 2002 (unpublished).
[6] S. G. Grubb *et al.*, Proceedings of Optical Amplifiers and Their Applications 1995, pp.197–199.
[7] J. D. Ania-Castañón, Opt. Express **12**, 4372 (2004).
[8] J. D. Ania-Castañón *et al.*, Phys. Rev. Lett. **96**, 023902 (2006).
[9] T. J. Ellingham *et al.*, IEEE Photon. Technol. Lett. **18**, 268 (2006).
[10] S. A. Babin *et al.*, Opt. Lett. **32**, 1135 (2007).
[11] J. Scheuer and A. Yariv, Phys. Rev. Lett. **97**, 140502 (2006).
[12] P.-L. Hsiung *et al.*, Opt. Express **12**, 5287 (2004).
[13] Y.-G. Han *et al.*, Opt. Lett. **30**, 1114 (2005).
[14] S. Huang *et al.*, Jpn. J. Appl. Phys. **42**, L1439 (2003).
[15] N. S. Kim, Rev. Laser Eng. Supplemental volume **2008**, 1115.
[16] H. A. Haus and M. Nakazawa, J. Opt. Soc. Am. B **4**, 652 (1987).
[17] S. A. Babin *et al.*, Opt. Lett. **31**, 3007 (2006).
[18] S. A. Babin *et al.*, J. Opt. Soc. Am. B **24**, 1729 (2007).
[19] V. E. Zakharov, V. S. L'vov, and G. Falkovich, *Kolmogorov Spectra of Turbulence* (Springer-Verlag, Berlin, 1992).
[20] S. A. Babin *et al.*, Phys. Rev. A **77**, 033803 (2008).
[21] Yu. S. Kivshar and G. P. Agrawal, *Optical Solitons: From Fibers to Photonic Crystals* (Academic Press, New York, 2003).
[22] P. Janssen, J. Phys. Oceanogr. **33**, 863 (2003).
[23] K. Trulsen and K. B. Dysthe, *Proceedings of the 21st Symposium of Naval Hydrodynamics* (National Academy of Sciences Press, Washington, DC, 1997).
[24] D. R. Solli *et al.*, Nature (London) **450**, 1054 (2007).
[25] J. M. Dudley, G. Genty, and B. J. Eggleton, Opt. Express **16**, 3644 (2008).